Adjoint-based model predictive control of wind farms
Beyond the quasi steady-state power maximization

Vali, Mehdi; Petrović, Vlaho; Boersma, Sjoerd; Wingerden, Jan Willem van; Kühn, Martin

DOI
10.1016/j.ifacol.2017.08.382

Publication date
2017

Document Version
Final published version

Published in
IFAC-PapersOnLine

Available online at www.sciencedirect.com

ScienceDirect

IFAC Papers Online CONFERENCE PAPER ARCHIVE

IFAC PapersOnLine 50-1 (2017) 4510–4515

Adjoint-based model predictive control of wind farms: Beyond the quasi steady-state power maximization ⋆

Mehdi Vali * **Vlaho Petrović** * **Sjoerd Boersma** **
Jan-Willem van Wingerden ** **Martin Kühn** *

* *ForWind, University of Oldenburg, Institute of Physics, Küpkersweg 70, 26129 Oldenburg, Germany, (e-mail: mehdi.vali@uni-oldenburg.de).*
** *Delft Center of Systems and Control, Delft University of Technology, Mekelweg 2, 2628 CD Delft, The Netherlands.*

Abstract: In this paper, we extend our closed-loop optimal control framework for wind farms to minimize wake-induced power losses. We develop an adjoint-based model predictive controller which employs a medium-fidelity 2D dynamic wind farm model. The wind turbine axial induction factors are considered here as the control inputs to influence the overall performance by taking wake interactions of the wind turbines into account. A constrained optimization problem is formulated to maximize the total power production of a given wind farm. An adjoint approach as an efficient tool is utilized to compute the gradient for such a large-scale system. The computed gradient is then modified to deal with the defined final set and practical constraints on the wind turbine control inputs. The performance of the wind farm controller is examined for a more realistic test case, a layout of a 2×3 wind farm with dynamical changes in wind direction. The effectiveness of the proposed approach is studied through simulations.

Keywords: Nonlinear model predictive control, Adjoint approach, Wind farm control, Wake interactions.

1. INTRODUCTION

Control of turbines within a wind farm is challenging because of their aerodynamic interactions via wakes. The characteristics of a wake are reduced wind speed and increased turbulence. The former reduces the total power production of the farm and the latter leads to a higher dynamic loading on the downstream turbines. The wake interactions depend strongly on the effects of different wind directions, local terrain, and turbine layout in a wind farm (Gebraad, 2014). Wind farm control has recently received much attention to lower the levelized cost of energy of wind farms, e.g., by minimizing the wake-induced power losses and structural fatigue loads through wind turbine control settings (Knudsen et al., 2015; Boersma et al., 2017).

Several studies have utilized optimization techniques to find the optimal set-points for the total wind farm performance (Gebraad et al., 2014; Marden et al., 2013; Gebraad and van Wingerden, 2015). Campagnolo et al. (2016a,b) have investigated the potential of different wind farm control strategies through wind tunnel testing. Vollmer et al. (2016) study the deflection of the wake by employing the yaw misalignment of upwind turbines in order to decrease wake losses of downwind turbines. Nonetheless, the approaches followed so far have been either open-loop or model-free ones. The inherent modeling uncertainties and time-varying inflow conditions, e.g. wind direction changes and wake meandering demand for a model-based closed-loop approach to react fast enough against sources of the wake interactions within a wind farm.

Soleimanzadeh et al. (2013) have developed a linear state-space model and a distributed controller for the wind farm, which is only valid for small deviations from the equilibrium. Goit and Meyers (2015) have proposed an optimal control of energy extraction, utilizing a Large Eddy Simulation (LES) model to increase the turbulent kinetic energy of inflow within a wind farm. The proposed controller relies on a full high-fidelity LES model to compute the optimal control commands, which is time-consuming for real-time control.

We developed a closed-loop optimal control framework for wind farms, the so-called adjoint-based model predictive control (AMPC), to optimize the performance with time-varying changes of the atmospheric conditions (Vali et al., 2016). It is designed based on WFSim, a control-oriented dynamic medium-fidelity wind farm model, which captures the dominant inflow dynamics in a computationally inexpensive manner. In this paper, we study our predictive control framework from a control engineering perspective. The computed adjoint-based gradient is modified to apply a specified final set and practical constraints on the wind turbine control inputs. Furthermore, we evaluate our approach for a layout example of a 2×3 wind farm with changes in wind direction, that changes wake interactions dynamically among wind turbines within the wind farm.

The remainder of this paper is organized as follows. In Section 2, we present briefly the fundamentals of WFSim. The main focus of Section 3 is on the structure of the proposed AMPC for wind farms. The explained methodology is discussed in Section 4 through simulation studies. Finally, the conclusions and outlook of this paper are presented in Section 5.

⋆ This work has been funded by the Ministry for Sciences and Culture of the Federal State of Lower Saxony, Germany as part of the PhD Programme on System Integration of Renewable Energies (SEE) and by the German Ministry of Economic Affairs and Energy (BMWi) in the scope of the WIMS-Cluster project (FKZ 0324005).

2405-8963 © 2017, IFAC (International Federation of Automatic Control) Hosting by Elsevier Ltd. All rights reserved.
Peer review under responsibility of International Federation of Automatic Control.
10.1016/j.ifacol.2017.08.382

2. WIND FARM MODEL

This section presents the fundamentals of the model used, which is a control-oriented dynamic medium-fidelity wind farm model: WFSim. The wind flow is modeled using the 2D Navier Stokes equations constrained by the continuity equation:

$$\rho\frac{\partial u}{\partial t}+\rho\nabla(u\mathbf{u})=-\frac{\partial p}{\partial x}+\nabla(\mu\nabla u)+S_x+T_x, \quad (1)$$

$$\rho\frac{\partial v}{\partial t}+\rho\nabla(v\mathbf{u})=-\frac{\partial p}{\partial y}+\nabla(\mu\nabla v), \quad (2)$$

$$\rho\nabla(\mathbf{u})=0, \quad (3)$$

where ρ is the air density, μ is the viscosity, p is the pressure field and $\mathbf{u}=[\mathrm{u},\mathrm{v}]$ is the velocity vector field at hub-height. S_x represents the external source terms in the x-direction, employed for incorporating the wind turbine models. The term T_x represents the turbulence model in WFSim, which uses Reynold's stress tensor according to the mixing length hypothesis (Boersma et al., 2016a). The set of equations (1)-(3) are spatially discretized, using the Hybrid differencing scheme, over a staggered grid of $(N_x \times N_y)$ cells. Furthermore, the implicit differencing scheme is employed to discretize the flow model temporally for the unsteady solution.

A wind turbine is modeled using actuator disc theory to exert a thrust force into the incoming flow and extract a certain amount of power from the wind. The thrust force and the produced power for a single turbine are expressed as follows (Gasch and Twele, 2011):

$$F_T=\frac{1}{2}\rho A_d U_\infty^2 C_T(a), \qquad C_T(a)=4a(1-a), \quad (4)$$

$$P_T=\frac{1}{2}\rho A_d U_\infty^3 C_P(a), \qquad C_P(a)=4a(1-a)^2, \quad (5)$$

where U_∞ is the effective wind speed at a far distance upwind from the rotor disc, A_d the swept area of the rotor plane, C_T and C_p are the thrust and power coefficients of the turbine respectively, which are functions of the axial induction factor a. The latter is a measure of the decrease in the stream-wise flow velocity at the rotor plane, which is combined with a first-order lag to model the wind turbine dynamic inflow as follows

$$\dot{a}=\frac{1}{\tau}(a_c-a), \quad (6)$$

where a_c is the wind turbine control command and τ represents the aerodynamic time constant.

Considering the induction effect of a rotor disc as

$$U_d=(1-a)U_\infty \quad (7)$$

enables us to estimate the exerted thrust force using the measurable wind velocity U_d at the rotor plane and the axial induction factor. Therefore, the i^{th} turbine model is incorporated inside the flow model (1) as follows

$$S_{x_i}=F_{T_i}=2\rho A_d U_{d_i}^2\beta_i, \qquad \beta_i=\frac{a_i}{1-a_i}, \quad (8)$$

where the virtual control variable β_i is defined to obtain a linear expression of the thrust force with respect to the wind turbine control setting. Finally, the wind farm model over a specified staggered grid can be represented in a nonlinear descriptor state-space form as follows

$$E(X_k)X_{k+1}=AX_k+B(X_k)\beta_k+b(X_k), \quad (9)$$

where

$$X_k=\begin{bmatrix}\bar{u}_k\\ \bar{v}_k\\ \bar{p}_k\end{bmatrix}, \quad \beta_k=\begin{bmatrix}\beta_{1,k}\\ \vdots\\ \beta_{N_t,k}\end{bmatrix}\in\mathbb{R}^{N_t\times 1},$$

and $\bar{u}_k\in\mathbb{R}^{(N_x-3)(N_y-2)\times 1}$, $\bar{v}_k\in\mathbb{R}^{(N_x-2)(N_y-3)\times 1}$ and $\bar{p}_k\in\mathbb{R}^{(N_x-2)(N_y-2)\times 1}$ are the vectors that stack all the velocities and pressures in every point of the staggered grid at the time instant k. The matrix $E(X_k)$ represents the spatial discretization terms of the x and y-momentum and the continuity equations (1)-(3). The constant matrix A is referred to as the temporal discretization of the flow depending on the chosen sampling time and the matrix $B(X_k)$ represents the linear expression of the thrust force with respect to the virtual control input β_k for the N_t number of wind turbines. Finally the matrix $b(X_k)$ represents the effect of the zero stress boundary conditions. An important feature of WFSim is the sparsity in the system matrices, improving the computational efficiency of such a large-scale dynamic system.

The power production of the i^{th} turbine within a wind farm can also be represented as a function of the wind speed at the rotor disc U_{d_i} and its own induction factor as follows

$$P_{T_i}=2\rho A_d U_{d_i}^3\beta_i. \quad (10)$$

See (Boersma et al., 2016a,b) for more details on the dynamic wind farm model and (Vali et al., 2016) on the implementation of the wind turbines as actuator discs.

3. ADJOINT-BASED MODEL PREDICTIVE CONTROL

We extend here our predictive control framework for wind farms (Vali et al., 2016) from a control engineering perspective, e.g., the practical constraints on the wind turbine control inputs. We modify the optimization problem and the way it is being solved in order to achieve more realistic wind farm peformance.

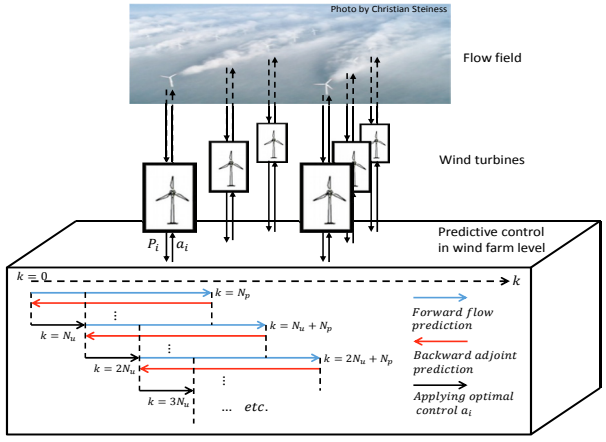

Fig. 1. Schematic illustration of the adjoint-based model predictive control (AMPC) of wind farms. Arrows show the control performance over time.

Figure 1 demonstrates schematically our proposed adjoint-based model predictive control (AMPC) framework for wind farms. It contains three main generic steps: prediction, solving an optimization problem over a finite time prediction horizon N_p and implementing the optimal control solutions over the receding time horizon $N_u \leq N_p$. The control inputs and plant responses are predicted in advance (see blue arrow in Fig. 1) and optimized for a finite time horizon N_p. The optimization

method benefits from an adjoint method as a cost-effective tool to compute the gradient of the specified performance index. Then, the adjoint field corresponding to the predicted flow (see red arrow in Fig. 1) is computed for estimating the proper search directions and solving the formulated optimization problem. Finally, the first part of the optimal solution is applied to the plant (see black arrow in Fig. 1). This procedure is repeated in the next controller sample time which provides the feedback into the optimization.

Here it is assumed that all required state variables for optimal control of a given wind farm are measurable. In order to avoid measuring the entire state variable, observation techniques could be employed. Doekemeijer et al. (2016) developed a computationally efficient Ensemble Kalman Filtering (EnKF) method for WFSim, which utilizes a limited amount of measurement points to reconstruct the mismatches between the 2D control-oriented wind farm model and a realistic wind plant simulation model, e.g., Simulator fOr Wind Farm Applications (SOWFA).

Furthermore, we only focus on the centralised structure of a high-level wind farm controller to find the optimal control setpoints of the wind turbines, taking their wake interactions into account. It is assumed that the low-level wind turbine control system, which is also an active field of research, provides the demanded active power control services to realize the overall goal (Fleming et al., 2016).

3.1 Optimization problem formulation

A constrained optimization problem is formulated here to minimize the wake-induced power losses within a wind farm. The manipulating variables are the wind turbine induction factors at time instant k defined as $\beta_k = [\beta_{1,k}, \beta_{2,k}, \dots, \beta_{N_t,k}]^T \in \mathbb{R}^{N_t \times 1}$. Note that we formulate the problem with respect to the virtual variable $\beta_i = \frac{a_i}{1-a_i}$ such that we have a linear expression of the thrust force with respect to the control input.

The optimal control problem is formulated as finding the maximal power production of the wind farm over a finite time horizon N_p. Hence, we first define the following performance index, referring to the total power production, at each time instant k as

$$\mathscr{J}_k(X_k, \beta_k) = \sum_{i=1}^{N_t} P_{i,k} \tag{11}$$

Now, we can formulate the following constrained optimization problem over the prediction horizon N_p

$$\max_{\tilde{\beta}} \quad \mathscr{J}(\tilde{X}, \tilde{\beta}) = \sum_{k=1}^{N_p} \mathscr{J}_k(X_k, \beta_k), \tag{12}$$

$$\text{s.t.} \quad \tilde{\mathbf{C}}(\tilde{X}, \tilde{\beta}) = 0, \tag{13}$$

$$\beta_{i,k} = \beta_{i,k-1} \quad , \quad k = N_p - N_f, \cdots, N_p \tag{14}$$

$$0 < \beta_{i,k} \leq 0.5, \tag{15}$$

The equality constraint (13) represents the spatial and temporal discretized inflow model, evolving over the prediction horizon N_p with the following expanded form

$$\tilde{\mathbf{C}} = \begin{bmatrix} C_1(X_0, X_1, \beta_0) \\ C_2(X_1, X_2, \beta_1) \\ \vdots \\ C_{N_p}(X_{N_p-1}, X_{N_p}, \beta_{N_p-1}) \end{bmatrix}, \quad \tilde{X} = \begin{bmatrix} X_1 \\ X_2 \\ \vdots \\ X_{N_p} \end{bmatrix}, \quad \tilde{\beta} = \begin{bmatrix} \beta_1 \\ \beta_2 \\ \vdots \\ \beta_{N_p} \end{bmatrix},$$

where according to (9)

$$\begin{aligned} C_k(X_{k-1}, X_k, \beta_{k-1}) = E(X_{k-1})X_k - AX_{k-1} \\ - B(X_{k-1})\beta_{k-1} - b(X_{k-1}) = 0. \end{aligned} \tag{16}$$

The terminal set constraints (14) is introduced to reduce the effects due to finite-time optimizations. The inequality constraint (15) also refers to practical constraints on the wind turbine control inputs.

3.2 Adjoint-based gradient of the cost function

Adjoint methods give an efficient way to obtain the gradient of a performance index when having many decision variables (Roth and Ulbrich, 2013). First, we define the *Lagrangian* to turn the constrained optimization problem (12)-(13) into the unconstrained one as follows

$$\mathscr{L}(\tilde{X}, \tilde{\beta}, \Lambda) \quad \equiv \mathscr{J}(\tilde{X}, \tilde{\beta}) + \Lambda^T \tilde{\mathbf{C}}(\tilde{X}, \tilde{\beta}), \tag{17}$$

where in this context Λ is the vector of *Lagrange multipliers*. Since the equality constraint (13) holds everywhere for $k = 1, 2, \cdots, N_p$, we may choose Λ freely. Therefore, the gradient of the cost function can be expressed in the following matrix form

$$\nabla_{\tilde{\beta}} \mathscr{J} \quad = (\mathscr{J}_{\tilde{X}} + \Lambda^T \tilde{\mathbf{C}}_{\tilde{X}}) \tilde{X}_{\tilde{\beta}} + \mathscr{J}_{\tilde{\beta}} + \Lambda^T \tilde{\mathbf{C}}_{\tilde{\beta}}, \tag{18}$$

where $(.)_{\tilde{X}}$ and $(.)_{\tilde{\beta}}$ represent the partial derivatives with respect to $\tilde{X}$ and $\tilde{\beta}$, respectively. Appendix A presents the sparse structure of $\tilde{\mathbf{C}}_{\tilde{X}}$ in (A.1) and $\tilde{\mathbf{C}}_{\tilde{\beta}}$ in (A.2) for a prediction window, constructed with the linearized model of WFSim around an equilibrium point at time instant k.

In order to avoid tedious computation of $\tilde{X}_{\tilde{\beta}}$, one may choose the adjoint field as a solution of the adjoint equation (Roth and Ulbrich, 2013):

$$\tilde{\mathbf{C}}_{\tilde{X}}^T(\tilde{X}, \tilde{\beta})\Lambda = -\mathscr{J}_{\tilde{X}}^T(\tilde{X}, \tilde{\beta}) \tag{19}$$

The structure of the adjoint equation (19) indicates that the adjoint field strongly depends on the definition of the performance index $\mathscr{J}$ and the wind farm model $\tilde{\mathbf{C}}$ over the prediction horizon. By substituting the adjoint field Λ into (18), there is no need for tedious calculation of the derivatives of the flow solution with respect to the control variables ($\tilde{X}_{\tilde{\beta}}$) and the gradient of the performance index can be expressed in the following compact form

$$\nabla_{\tilde{\beta}} \mathscr{J} = \mathscr{J}_{\tilde{\beta}}(\tilde{X}, \tilde{\beta}) + \Lambda^T \tilde{\mathbf{C}}_{\tilde{\beta}}(\tilde{X}, \tilde{\beta}). \tag{20}$$

Exploiting the sparse structure of the matrices $\tilde{\mathbf{C}}_{\tilde{X}}$ in (A.1) and $\tilde{\mathbf{C}}_{\tilde{\beta}}$ in (A.2), one can derive the time-propagation of the adjoint field (19) and the gradient (20) as follows

$$(C_{k-1})_{X_{k-1}}^T \lambda_{k-1} = -\mathscr{J}_{X_{k-1}}^T(\tilde{X}, \tilde{\beta}) - (C_k)_{X_{k-1}}^T \lambda_k, \tag{21}$$

$$\nabla_{\beta_{k-1}} \mathscr{J} = \mathscr{J}_{\beta_{k-1}}(\tilde{X}, \tilde{\beta}) + \lambda_k^T (C_k)_{\beta_{k-1}}. \tag{22}$$

with initializing $\lambda_{N_p+1} = 0$.

3.3 Control input constraints

Recalling the formulated optimization problem (12)-(15), we modify the computed adjoint-based gradient to apply the specified constraints (14) and (15) on the wind turbine control inputs. At the end of the horizon, the constraint (14) tries to reduce

the terminal undesired moves due to the generic effects of the finite-time optimization problem. We introduce the following mapping of the computed gradient of the i^{th} turbine to mitigate this effect:

$$\bar{\nabla}_{\beta_i} \mathscr{J} = \nabla_{\beta_i} \mathscr{J} \mathbf{T}, \quad \mathbf{T} = \begin{bmatrix} I_{N_p - N_f} & 0 \\ 0 & [1]_{N_f \times 1} \end{bmatrix}. \tag{23}$$

We also employ an active set method combined with a line-search to restrict the control inputs at each sample time to the specified limits (15). The line-search method is employed here to guarantee the new estimation in the computed search direction lies within the high-dimensional feasible region. When a constraint is activated, e.g., $\beta_{i,k} = 0.5$ or $\beta_{i,k} = 0$, the search direction moves along the activated constraint.

3.4 Optimization method

Given an estimated control variable $\tilde{\beta}^{(n)} \in \mathbb{R}^{N_t N_p \times 1}$ at the n^{th} optimization iteration, a new estimation is obtained using the modified search direction (23) as follows

$$\tilde{\beta}^{(n+1)} = \mathbf{T} \bar{\nabla}^{(n)}_{\tilde{\beta}} \mathscr{J}^T + \tilde{\beta}^{(n)}, \tag{24}$$

where the transformation matrix $\mathbf{T}$ applies the final set constraints (14) to the new estimation. A backtracking line search based on the Armijo rule (Bertsekas, 2004) is employed to find iteratively a step size that determines how far control variables should move along the search direction, leading to improvement in the total power production of the wind farm.

4. SIMULATION STUDIES

The performance of the adjoint-based model predictive controller is shown here through simulation studies with time-varying atmospheric conditions. A layout of a 2×3 wind farm is considered (see Fig. 2) and simulated with WFSim. The wind turbines with rotor diameter $D = 126$ m are spaced $5D$ in the stream-wise direction. The rotor centers of the middle turbines are misaligned half a rotor diameter from the centers of the upwind and downwind turbines. We have a field of 3000×2000 m^2 with a staggered grid of 100×75 cells ($N_x \times N_y$). Here, the flow is simulated for laminar flow conditions, where viscous forces are dominant. The simulation is started with an uniform wind field with $u = 10$ m/s and $v = 0$ m/s.

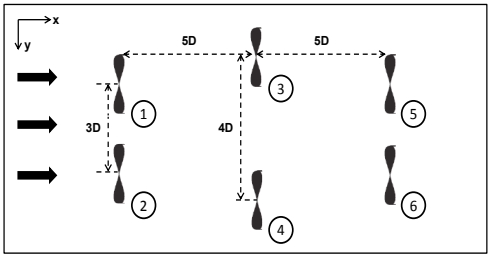

Fig. 2. The layout of the simulated 2×3 wind farm.

We consider the performance of the controller in the below-rated region, where the wind speed is lower than its rated value. The main control objective here is to operate at the optimal point on a wind farm level, i.e., capturing the kinetic energy of wind as much as possible. Although this optimal point is unique with respect to the different wind speeds at this region, it varies with changes in the wind direction due to different induced wake interactions among the wind turbines. Hence, the wind farm controller must be able to adjust the control inputs in such a way that the wind farm always operates at the corresponding optimum point. The AMPC is examined here to find the optimal wind turbines' induction factors while the wind direction changes over time, yielding up to 8° misalignment with the rotors of the turbines.

4.1 Optimal references

To evaluate the performance of the AMPC, we first search for the optimal control settings for two different wind farm operating conditions, full and partial wake interactions. First, we assume that the inflow is aligned to the rotor discs and wind turbines interact fully through their wakes. Second, the incoming wind is misaligned 8° with the rotor discs due to a wind direction change, that mitigates aerodynamic interactions of the wind turbines. We employed a Game Theoretic (GT) approach, an open-loop control strategy, proposed for maximizing the power production of wind farms in an iterative procedure (Marden et al., 2013).

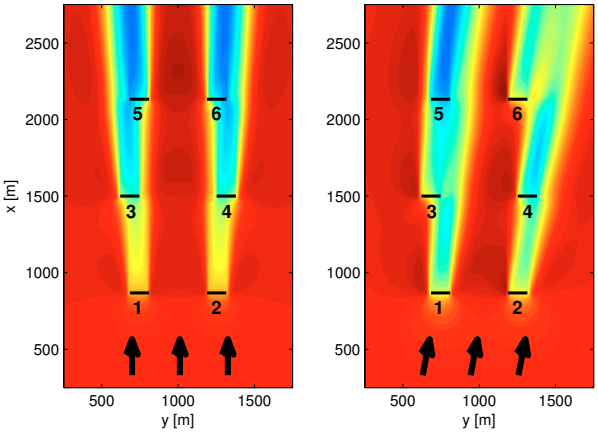

Fig. 3. Six-turbine example operating with the optimal axial induction factors, achieved using GT approach, at $U_\infty = 10$ m/s. The incoming flow is aligned to the rotor discs (left) and misaligned 8° with the rotor discs (right), resulting in full and partial wake interactions, respectively.

Figure 3 depicts our six-turbine example operating with the optimal axial induction factor at ambient wind speed $U_\infty = 10$ m/s for two different wind farm operating conditions, i.e., the full wake (left) and the partial wake (right) interactions. The corresponding optimal control settings, achieved by the GT approach after almost 400 iterations, are listed in Table 1. It should be noted that the asymmetric coordination of the induction factors for the partial wake relates to the amount of wake deflections from downstream turbines, caused by the 8° wind direction change (see the right plot of Fig. 3). The simulation results with WFSim show that there exists the potential of an 8 % power increase for the full wake conditions and a 2 % increase for the partial wake conditions, with respect to the greedy control, via the optimal coordination of the wind turbine control settings.

4.2 Power maximization with dynamical changes in wind direction

In order to evaluate the performance of the AMPC, the following simulation scenario is defined. The wind farm starts

Table 1. Steady-state optimal set-points of wind turbines, achieved using GT approach, for two different wind directions.

Full-wake (0°)		Partial-wake (8°)	
a_1 =0.16	a_2 =0.16	a_1 =0.31	a_2 =0.27
a_3 =0.25	a_4 =0.25	a_3 =0.25	a_4 =0.27
a_5 =0.31	a_6 =0.31	a_5 =0.29	a_6 =0.31

operating with the optimal axial induction factors, at the ambient wind speed 10 m/s while the wind direction is aligned to the rotor discs (see the left plot of Fig. 3). After 600 s we change the wind direction at the boundary conditions yielding 8° misalignment with rotor discs after propagation (see the right plot of Fig. 3). After 600 additional seconds, the wind turns again into the initial direction. The simulation sample time and the aerodynamic time constant of each turbine are selected as Δt =2 s and τ =13.5 s (Vali et al., 2016).

The key parameters of the AMPC are chosen here as the prediction horizon N_p =600 s, the receding horizon N_u =60 s, and the final time period N_f =60 s. There exist two significant criteria for choosing the prediction horizon N_p. It should be long enough to predict the inflow propagation within a wind farm and also to avoid penetrating the transition behaviour of the adjoint variable (21) at the end of the horizon. The final time period N_f is introduced and chosen to reduce the latter effect. The controller sample time N_u depends on how fast the wind farm dynamics change.

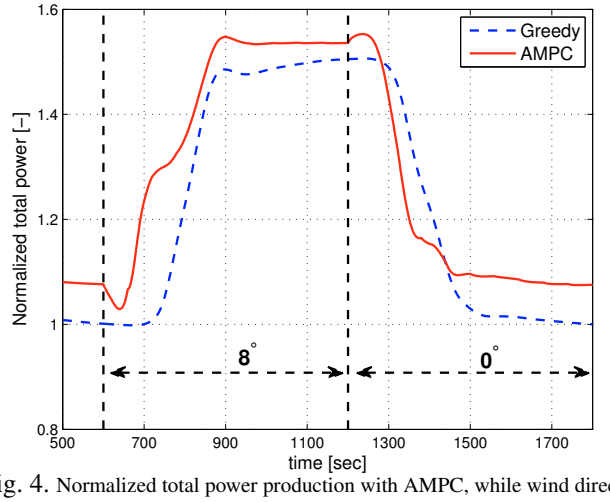

Fig. 4. Normalized total power production with AMPC, while wind direction changes. The power is normalized with respect to the total power of the greedy control at the full-wake operating condition.

Figure 4 shows the optimal control of the energy extraction of our simulated example with wind direction changes, compared with the greedy control (a_i =0.33). It can be seen that the AMPC is able to maximize the power production, while its optimal operating point is altered due to changes in the atmospheric conditions. The controller relatively reacts fast, because the control inputs and wind farm responses are predicted in advance and optimized with respect to the total power production. After applying the optimal control commands during the control horizon N_u =60 s, the wind farm responses to the control inputs and disturbances, e.g., changes in the wind direction, are fed back to the controller and then the optimal control inputs are adjusted at the next prediction and optimization window.

Figure 5 illustrates the time-varying behaviour of the axial induction factors of the first (upper plot) and the second (lower plot) row. Only the two first machines of each row are shown here. The control inputs converge fast to the optimal references (green lines), obtained by the GT approach (see Table 1). The last machines, i.e., 5th and 6th turbines, are operating almost at the greedy control setting to capture the most possible kinetic energy from the incoming wind.

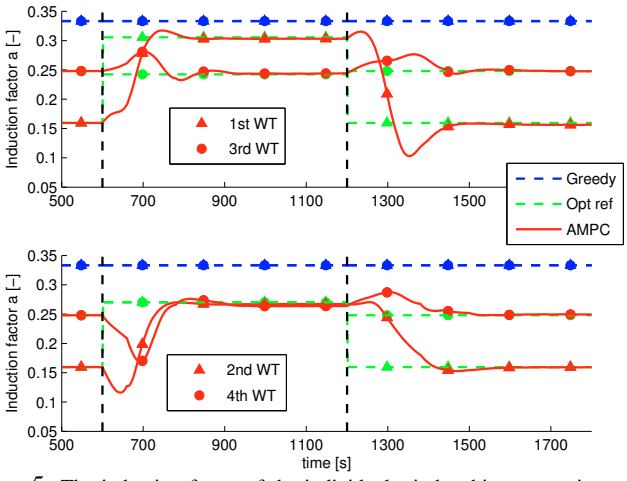

Fig. 5. The induction factor of the individual wind turbines operating with AMPC, compared with the greedy control a_i = 0.33: (upper) 1st and 3rd turbines; (lower) 2nd and 4th turbines. Green lines represent the steady-state optimal set-points of the wind turbines, computed by GT approach (Table 1).

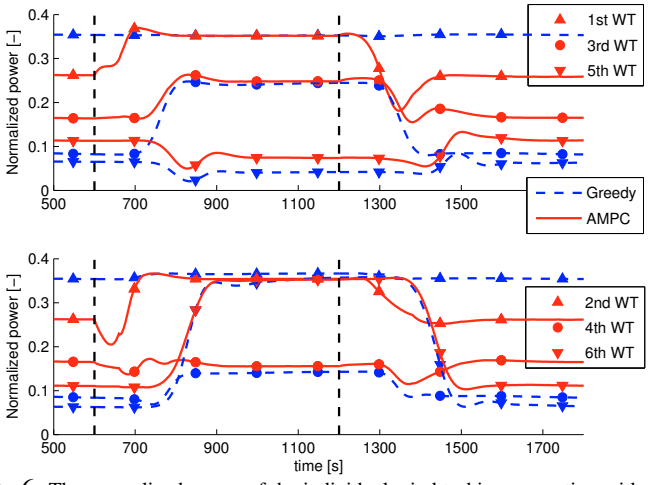

Fig. 6. The normalized power of the individual wind turbines operating with AMPC, compared with the greedy control: (upper) 1st row; (lower) 2nd row of the wind turbines. The power is normalized with respect to the total power of the greedy control at the full-wake operating condition.

Figure 6 illustrates the normalized power production of each wind turbine. The optimal power production when the inflow has 8° misalignment with the rotor area is almost in the same level of the greedy control due to less power losses caused by partial wake interactions. This misalignment might redirect a turbine's wake downstream and consequently affect the performance of the downwind turbine. For instance, the noticeable power increases of the 3rd and 6th machines are due to the wake deflections of their upwind turbines (see the right plot of Fig. 3).

While the wind turbines are fully interacting through wakes (last 10 min), AMPC reduces the energy extraction of the upwind turbines to increase the kinetic energy of the inflow downstream and consequently to maximize the total power production of the downwind turbines. It can be seen that the

most of the power gains of the wind farm (last 10 min) are achieved by the 5th and 6th wind turbines due to the optimal coordination of the induction factors.

5. CONCLUSION

The fundamentals of our adjoint-based model predictive control framework for optimal energy extraction of wind farms are presented and extended from some practical perspectives. A constrained optimization problem is formulated and an adjoint method is employed to compute the gradient of the determined performance index in a computationally effective manner. Since the performance index is considered here for the optimal energy extraction for wind farms, it can be adapted and applied for any size and type of wind turbines. The effectiveness of the closed-loop wind farm controller is examined using a layout example of a 2×3 wind farm, with dynamical changes in wind direction. Simulation results show that the AMPC is able to converge to the optimal control set-points through feedback, while the atmospheric conditions change. In the future, we implement the AMPC over a Large Eddy Simulation (LES) model with more detailed wind farm inflow dynamics in order to assess its performance with more realistic time-varying atmospheric conditions, e.g., turbulent wind and wake meandering.

ACKNOWLEDGEMENTS

The main author specially wants to thank Lucy Y. Pao for the insightful discussions and her valuable remarks on this work.

REFERENCES

Bertsekas, D. (2004). *Nonlinear Programming*. Athena Scientific.

Boersma, S., Doekemeijer, B.M., Gebraad, P.M.O., Fleming, P.A., Annoni, J., Scholbrock, A.K., Frederik, J.A., and van Wingerden, J.W. (2017). A tutorial on control-oriented modelling and control of wind farms. *American Control Conference (ACC), 2017*.

Boersma, S., Gebraad, P.M.O., Vali, M., Doekemeijer, B., and van Wingerden, J.W. (2016a). A control-oriented dynamic wind farm flow model: WFSim. In *Journal of Physics: Conference Series*, volume 753, 032005. IOP Publishing.

Boersma, S., Vali, M., Kühn, M., and van Wingerden, J.W. (2016b). Quasi linear parameter varying modeling for wind farm control using the 2D Navier-Stokes equations. In *American Control Conference (ACC), 2016*, 4409–4414.

Campagnolo, F., Petrović, V., Bottasso, C.L., and Croce, A. (2016a). Wind tunnel testing of wake control strategies. In *American Control Conference (ACC), 2016*, 513–518.

Campagnolo, F., Petrović, V., Schreiber, J., Nanos, E.M., Croce, A., and Bottasso, C.L. (2016b). Wind tunnel testing of a closed-loop wake deflection controller for wind farm power maximization. In *Journal of Physics: Conference Series*, volume 753, 032006. IOP Publishing.

Doekemeijer, B., van Wingerden, J.W., Boersma, S., and Pao, L.Y. (2016). Enhanced Kalman filtering for a 2D CFD NS wind farm flow model. In *Journal of Physics: Conference Series*, volume 753, 052015. IOP Publishing.

Fleming, P., Aho, J., Gebraad, P.M.O., Pao, L.Y., and Zhang, Y. (2016). Computational fluid dynamics simulation study of active power control in wind plants. In *American Control Conference (ACC), 2016*, 1413–1420.

Gasch, R. and Twele, J. (2011). *Wind power plants: fundamentals, design, construction and operation*. Springer Science & Business Media.

Gebraad, P.M.O., Teeuwisse, F., van Wingerden, J.W., Fleming, P., Ruben, S., Marden, J., and Pao, L.Y. (2014). Wind plant power optimization through yaw control using a parametric model for wake effects: a CFD simulation study. *Wind Energy*, 19(1), 95–114.

Gebraad, P.M.O. and van Wingerden, J.W. (2015). Maximum power-point tracking control for wind farms. *Wind Energy*, 18(3), 429–447.

Gebraad, P.M.O. (2014). *Data-driven wind plant control*. Ph.D. thesis, TU Delft, Delft University of Technology.

Goit, J.P. and Meyers, J. (2015). Optimal control of energy extraction in wind-farm boundary layers. *Journal of Fluid Mechanics*, 768, 5–50.

Knudsen, T., Bak, T., and Svenstrup, M. (2015). Survey of wind farm control power and fatigue optimization. *Wind Energy*, 18(8), 1333–1351.

Marden, J.R., Ruben, S.D., and Pao, L.Y. (2013). A model-free approach to wind farm control using game theoretic methods. *IEEE Transactions on Control Systems Technology*, 21(4), 1207–1214.

Roth, R. and Ulbrich, S. (2013). A discrete adjoint approach for the optimization of unsteady turbulent flows. *Flow, turbulence and combustion*, 90(4), 763–783.

Soleimanzadeh, M., Wisniewski, R., and Johnson, K. (2013). A distributed optimization framework for wind farms. *Journal of Wind Engineering and Industrial Aerodynamics*, 123, 88–98.

Vali, M., van Wingerden, J.W., Boersma, S., Petrović, V., and Kühn, M. (2016). A predictive control framework for optimal energy extraction of wind farms. In *Journal of Physics: Conference Series*, volume 753, 052013. IOP Publishing.

Vollmer, L., Steinfeld, G., Heinemann, D., and Kühn, M. (2016). Estimating the wake deflection downstream of a wind turbine in different atmospheric stabilities: an LES study. *Wind Energy Science*, 1(2), 129–141. doi: 10.5194/wes-1-129-2016.

Appendix A. PARTIAL DERIVATIVES OF THE WIND FARM MODEL AT ONE PREDICTION HORIZON

The derivatives of the discretized wind farm model $\tilde{\mathbf{C}}(\tilde{X},\tilde{\beta})=0$ with respect to the state $\tilde{X}$ and control input $\tilde{\beta}$, over the whole prediction horizon N_p:

$$\tilde{\mathbf{C}}_{\tilde{X}} = \begin{bmatrix} (C_1)_{X_1} & 0 & \cdots & 0 & 0 \\ (C_2)_{X_1} & (C_2)_{X_2} & \cdots & 0 & 0 \\ \vdots & \ddots & \ddots & \vdots & \vdots \\ 0 & 0 & \ddots & (C_{N_p-1})_{X_{N_p-1}} & 0 \\ 0 & 0 & \cdots & (C_{N_p})_{X_{N_p-1}} & (C_{N_p})_{X_{N_p}} \end{bmatrix} \tag{A.1}$$

$$\tilde{\mathbf{C}}_{\tilde{\beta}} = \begin{bmatrix} 0 & 0 & \cdots & 0 & 0 & 0 \\ (C_2)_{\beta_1} & 0 & \cdots & 0 & 0 & 0 \\ 0 & (C_3)_{\beta_2} & \cdots & 0 & 0 & 0 \\ \vdots & \vdots & \ddots & \vdots & \vdots & \vdots \\ 0 & 0 & \cdots & (C_{N_p-1})_{\beta_{N_p-2}} & 0 & 0 \\ 0 & 0 & \cdots & 0 & (C_{N_p})_{\beta_{N_p-1}} & 0 \end{bmatrix} \tag{A.2}$$